XPS Study of Interface and Ligand Effects in Supported Cu_2O and CuO Nanometric Particles

J. Morales, J. P. Espinos, A. Caballero, and A. R. Gonzalez-Elipe*

Instituto de Ciencia de Materiales de Sevilla (CSIC-University Sevilla) and Dpt. Q. Inorganica, Avda. Americo Vespucio s/n, 41092 Sevilla, Spain

Jose Antonio Mejias

Departamento de Ciencias Ambientales, Universidad Pablo de Olavide, Ctra Utrera km 1, E−41013 Sevilla, Spain

Received: October 14, 2004; In Final Form: March 2, 2005

This paper reports an analysis of the changes in the photoemission parameters of copper in small particles of copper oxides deposited on silicon dioxide. This study is of relevance for investigations in the fields of heterogeneous catalysis and coordination chemistry. Copper oxides (Cu_2O and CuO) have been deposited on the surface of a flat SiO_2 substrate by evaporation of copper and subsequent oxidization of the deposited particles. XPS has been used to analyze the chemical and coordination state of copper. Large variations in the Cu $2p_{3/2}$ binding energy (BE) and Auger parameter (α') have been found as a function of the type and amount of deposited copper oxide. The differences in BE calculated from the values of the lowest amount of deposited material and those of the bulk compounds were −0.4 eV (Cu_2O) and −1.9 eV (CuO), while those in α' amounted to 2.9 (Cu_2O) and 1.6 eV (CuO). The observed changes have been described in terms of the chemical state vector (CSV) concept in a Wagner plot and rationalized by considering the characteristics of bonding and electronic interactions that occur at a given oxide/oxide interface. These interactions have been modeled by means of quantum mechanical calculations with cluster models simulating the Cu−O−Si bonding at the interface. The effect of the polarization of the surrounding media around the copper cations has been also estimated for both the dispersed clusters supported on the SiO_2 substrate and for the copper oxide materials in bulk form. A change in the values of α' and BE of copper (ie., $\Delta\alpha' = 1.1$ eV, $\Delta BE = 0.1$ eV) upon adsorption on the Cu^+ species of Cu_2O moieties dispersed on SiO_2 of a phenyl-acetylene molecule illustrates the use of XPS to study the formation of cation−ligand complexes in heterogeneous systems. A detailed description of the bonding interactions of these coordinated Cu^+ species in terms of initial and final state effects of the photoemission process has been also carried out by means of quantum mechanical calculations and cluster models.

Introduction

One of the most useful concepts in X-ray photoemission spectroscopy (XPS) is the Auger parameter (α').[1] This parameter can be related to the extra-atomic relaxation energy of photoholes in the final state of the atoms undergoing photoemission. It depends on the electronic and dielectric properties of the environment around the photoexcited atom. Recently, Moretti[2] has proposed a model that correlates the magnitude of $\Delta\alpha'$ (i.e., the difference in α' for a given atom in a compound with respect to the same atom in a reference material) with the polarizability and the number of ligands around the photoemitting atom. Within this context, we have also studied by XPS the changes in binding energy (BE) of the photoemission peaks and in the α' parameter of a cation when an oxide of that element is deposited on another oxide acting as support.[3] A rather general behavior for many oxide/oxide couples was that the BE decreases and α' increases, or vice versa, with the amount of deposited material. In this way, only for large amounts of the deposited oxide, when the layer is relatively thick, values similar to those of the bulk compounds are obtained. These changes in the electronic parameters of the cations pertaining to small moieties of the deposited oxide were correlated with both the type of interactions appearing at the interface and with the different polarization of the system due to the distinct dielectric constants of the substrate and supported phases.[4] A correlation of such behavior with some macroscopic, chemical, and physical properties, of the system has been also studied in a few works (e.g., chemical reactivity of supported oxide catalysts,[5] change in the refraction index of related mixed oxide compounds,[6] etc.).

Copper oxide (i.e., CuO and Cu_2O) compounds are interesting materials because of their use as catalysts, interconnects in electronics, corrosion of alloys,[7−9] etc. The identification of the actual oxidation state of copper in these systems is critical to understand their chemical behavior and physical properties. Usually, the attribution of oxidation states of this element is done by considering both the Cu 2p photoemission peaks and the Cu L_3VV Auger peak. In particular, the use of these two peaks is necessary if Cu^+ has to be differentiated from Cu^0.[10] When copper oxides are dispersed on the surface of another oxide support, the electronic parameters of the Cu^{2+} or Cu^+ species (i.e., BE and α') may undergo significant changes. In a previous publication, these changes have been analyzed as a

* Corresponding author. E-mail arge@icmse.csic.es.

10.1021/jp0453055 CCC: $30.25
Published on Web 04/05/2005

function of the dispersion degree of the corresponding oxides supported on ZrO_2 and SiO_2.[11] Also, for copper exchanged zeolites, the changes in the electronic parameters of copper have been discussed using the Auger parameter concept.[12]

With the present work, we want to go a step forward in the study of solids with deposited speciesby using an experimental approach close to that of the coordination chemistry. XPS has been previously used to study coordination compounds,[13−14] but no systematic use has been made when these coordination compounds are supported on a substrate or formed on it by adsorption of ligand molecules. In the present work, we discuss the type of interactions responsible for the changes in the electronic parameters of Cu^+ and Cu^{2+} species in nanometric Cu_2O and CuO particles dispersed on SiO_2. We also describe theoretically these interactions by means of quantum mechanical calculations with cluster models. A similar approach, consisting of the use of the Auger parameter and the chemical state vector (CSV)[15] concepts, has been also applied to describe the bonding effects found upon adsorption of a phenylacetylene (PA) ligand on the Cu^+ species of Cu_2O moieties deposited on SiO_2.

Experimental Section and Methods

Cu_2O or CuO were deposited on a SiO_2 flat substrate (an oxidized layer of SiO_2 of 200 A grown on a Si substrate) by progressive evaporation of copper and subsequent exposure to oxygen (for Cu_2O) or to a plasma of oxygen (for CuO) at 298 K under well-defined conditions. A detailed description of the experimental conditions that enable a precise control of the stoichiometry of the oxides can be found in a previous publication.[11] XPS spectra were recorded in a ESCALAB 210 spectrometer from VG supplied with a preparation chamber (base pressure 10^{-8} Torrs) where all the evaporation and adsorption experiments were carried out. The spectra were recorded with the Mg Kα radiation in the constant pass energy mode with a value of 20 eV. The Si 2p peak of the Si^{4+} species of the SiO_2 substrate taken at 102.8 eV has been used as a reference for calibration of the BE scale. In this way, the small displacements (less than 1 eV) of the peaks in energy position due to charging effects were compensated. In some cases, when the difference in BEs between the peaks was very small, their exact position was determined by fitting a Gaussian curve to them. A maximum error bar of 0.05 eV can be estimated for the measurements.

The adsorption experiments of the phenyl-acetylene (PA) ligand were carried out in the prechamber of the spectrometer by dosing 1 mbar of this compound on a sample with a small amount of deposited Cu_2O moieties. The PA compound was first degassed by a series of pumping and condensation cycles at 77 K. After adsorption of the vapor, the chamber was pumped at room temperature up to achieve its ultimate residual pressure.

The energy and charge distribution of the different cluster models are calculated within the density functional theory (DFT)[16] and the B3LYP exchange-correlation potential.[17] For the calculation of the relaxation energies of the photoholes we make use of the $Z + 1$ approximation: the relaxation energy is calculated as the difference between the total energy of a cluster with a Cu atom and the energy of a cluster where Cu has been substituted by Zn^+. For these calculations we make use of the D95V Gaussian basis set for H, O and C[18] and Stuttgart/Dresden ECPs for Cu and Zn.[19] The changes in electron density around the atoms are estimated from the natural electron configurations.[20] For these calculations we use the 6-311++$G^{2d,2p}$ for all atoms. That includes the 6-311G basis for H, O and C[21] and

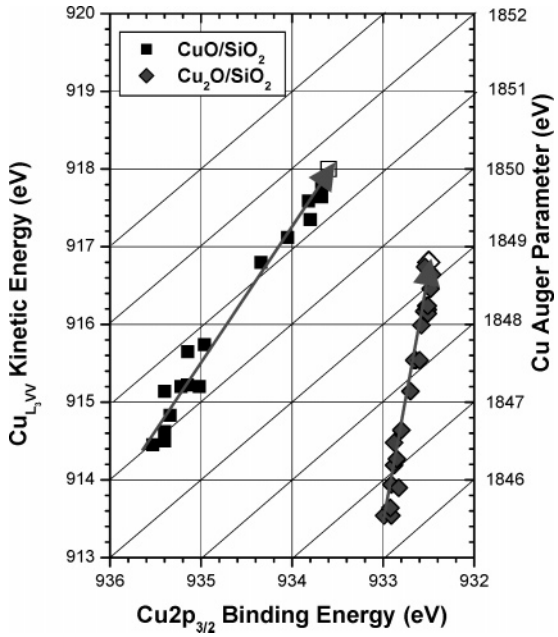

Figure 1. Wagner plot describing the changes in BE and α' for increasing amounts of Cu_2O and CuO deposited on SiO_2. The arrows are the CSVs for each oxide. The points with hollow signs correspond to the bulk oxides.

the Wachters−Hay[22,23] basis using the scaling factors of Raghavachari and Trucks[24] for Cu and Zn, as well as diffuse functions[25] and multiple polarization functions.[26] All the calculations are done with the Gaussian03 program.[27] The $z + 1$ approximation has been used previously for the relaxation energy in oxides,[4] but as far as we are aware, no calculations for copper oxides have been reported. Ab initio methods have been extensively used for the interpretation of XPS spectra of copper compounds (see for example ref 28).

Results

Cu 2p BE and Auger Parameter for Cu_2O and CuO Deposited on SiO_2. In a previous report we have described the evolution of the values of BE and α' for Cu^0, Cu^+, and Cu^{2+} species, when small particles or very thin layers of Cu, Cu_2O or CuO are deposited by evaporation on the surface of an oxide substrate.[11] As a result of these previous investigations we found that the BE of the Cu $2p_{3/2}$ photoelectron peak and the α'parameter of copper change continuously from the lowest coverage situation up to the value of the bulk materials. The change in BE and $\alpha'$of Cu^+ and Cu^{2+} species deposited in the form of the corresponding oxides on the surface of a SiO_2 substrate are represented in the form of a Wagner plot in Figure 1. In this figure, the points corresponding to the two bulk oxides are indicated as a hollow point. The different points in the plot represent the measured values for increasing amounts of each copper oxide. The arrows in this figure are the chemical state vectors (CSV) for each supported copper oxide. This vector has been defined to account in a simple way for variations as those depicted in this figure.[15] Its main advantage is that it provides a direct description of the variation range of the electronic parameters for a given MO/M′O system (MO and M′O mean the deposited and substrate oxides respectively). For that it is enough to indicate the coordinates of the origin of the vector since its tip is defined by the position of the point corresponding to bulk MO.[15] Thus, the components of the vector are defined

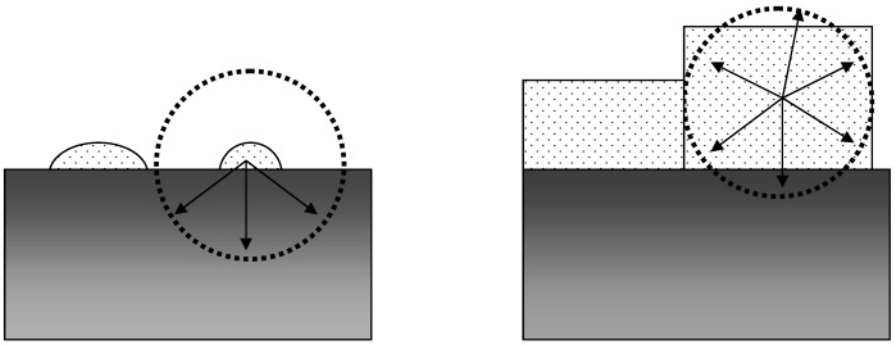

Figure 2. Scheme of polarization effects induced by a photohole in a nanoparticle at different stages of growth. The polarization contribution of the support to $\Delta\alpha'$ decreases when the size of the particle increases.

TABLE 1: Magnitude of the Total Experimental Variations of the Electronic Parameters of Cu^+ and Cu^{2+} for Cu_2O and CuO Deposited on SiO_2[a] (All Values in eV)[15]

system	ΔBE[b]	ΔKE[b]	ΔKE/ΔBE	$\Delta\alpha'$	ΔRE	$\Delta\epsilon$
CuO/SiO_2	−1.9	3.6	−1.9	1.6	0.8	−1.1
Cu_2O/SiO_2	−0.4	3.0_5	−7.6	2.9	1.4_5	1.10

[a] Variations have been calculated by subtracting in each experiment the values of the lowest coverage situation from those of the bulk compounds. [b] ΔBE and ΔKE are the *X* and *Y* components of the CSV.

as the difference in BE of photoelectron peaks and KE of the Auger peaks between the point corresponding to the bulk oxide minus that of the lowest coverage situation. For the two series of results represented in Figure 1, the coordinate values of the CSVs are summarized in Table 1.

This table, besides the change in experimental parameters (i.e., ΔBE, ΔKE and $\Delta\alpha'$) and in the slope of the CSV (i.e., ΔKE/ΔBE), includes the changes in extra-atomic relaxation energy of the photohole in the final state, ΔRE, and the change in the initial state energy of the system, $\Delta\epsilon$. The two latter magnitudes are calculated by the well-known expressions[29]

$$\Delta\mathrm{RE} = {}^1/_2\Delta\alpha' \tag{1}$$

$$\Delta\epsilon = \Delta\mathrm{BE} + \Delta\mathrm{RE} \tag{2}$$

RE arises when a photohole is suddenly created in an atom and accounts for the gain in energy of the system provided by the rearrangement of the free electrons (in the case of metals) or the dipoles (in the case of dielectric materials) of the medium to compensate the creation of such a hole. On the other hand, ϵ describes the energy of the system before photoemission and, for a given atom, differs depending on its density of charge and on the magnitude of the Madelung potential (MP) around it (i.e., number, type and charge of coordinating atoms). $\Delta\epsilon$ and ΔRE account for the changes in ϵ and RE for a given atom in two different chemical or electronic environments.

Polarization Contribution of the Interface to RE in Deposited Nanometric Particles. It has been pointed out that for systems consisting of a very thin film or small moieties of an oxide deposited on another oxide of different polarization characteristics (i.e., different value of their dielectric constants), there is a contribution to ΔRE due to the distinct polarization of the materials constituting the substrate and the deposited phase.[3,4] This contribution arises when the layer thickness or particles size of this latter is small and is due to the fact that the rearrangement and/or generation of dipoles by the photohole is different in the substrate than in the supported phase. A scheme of this situation is depicted in Figure 2. This figure also shows that for thicker films or big particles the supported phase can be considered as equivalent to the bulk, since in practice the substrate is not affected by the photohole. For very thin films or very small particles, the polarization contribution to ΔRE (and therefore $\Delta\alpha'$) can be estimated with the expression[4]

$$\Delta\alpha'_{\mathrm{p}} = 11.4/t[(1/n_{\mathrm{l}})^2 - (1/n_{\mathrm{s}})^2] \tag{3}$$

where t is the average thickness of the deposited layer or particle and n_{s} and n_{l} are the refraction indexes of the substrate and supported materials. Note that the dielectric constants can be approximated by n^2. Owing to the assumptions made for the development of this expression, it only accounts for the contribution to RE of the medium beyond the first coordination sphere around the cation.[4]

From this formula, the maximum polarization contributions to ΔRE ($\Delta\mathrm{RE}_{\mathrm{pol}} = \Delta\alpha'_{\mathrm{p}}/2$ is calculated from formula 3) estimated for the Cu_2O/SiO_2 and CuO/SiO_2 systems are, respectively, 0.55 and 0.35 eV. These values correspond to monolayerlike moieties where the polarization energy is mainly due to the support. Taking into account these values, the data in Table 1 can be modified to extract the actual variations in α' due to "chemical effects", i.e., α'_{Chem}. These are the changes in electronic parameters associated with a modification of the nearest chemical environment around copper (i.e., first coordination sphere) when the cations of the first monolayer are bonded to the silica substrate trough some bridging oxygen ions. For the copper ions in direct interaction with the silica it is expected that the oxygen atoms around it are different than for the oxygen ions bonded to copper in the bulk oxide and that, therefore, the Cu−O bonds are not totally equivalent for the two situations. The changes in α' due to chemical bonding at the interface can be calculated according to

$$\Delta\alpha'_{\mathrm{Chem}} = \Delta\alpha' - \Delta\alpha'_{\mathrm{p}}$$

The changes in the rest of electronic parameters due to bonding interactions can be calculated from Table 1. The resulting values are summarized in Table 2.

The visualization of the different contributions considered in this analysis can be done in a Wagner plot by means of the CSV concept as illustrated in Figure 3. This figure summarizes, in the form of a vector, the whole set of experimental results represented in Figure 1 for Cu_2O and CuO. Besides the experimental vectors **AB**, this figure depicts the vectors **AA′** that account for the $\Delta\alpha_{\mathrm{p}}'$ contributions. The difference vectors **A′B**, calculated by subtracting the polarization from the experimental vector, are the vectors accounting for chemical and electronic effects arisen by the interaction of the copper oxide and the SiO_2 substrate. The coordinates of these new vectors are summarized in Table 2 (i.e., ΔBE(chem) and ΔKE(chem)). The position of the origin of these vectors describe

TABLE 2: Magnitude of the Variations in Electronic Parameters Due to Chemical Interactions for Cu_2O and CuO Deposited on SiO_2 (All Values in eV)

system	ΔBE_{Chem}	ΔKE_{Chem}	$\Delta KE/\Delta BE$ (chem)	$\Delta\alpha'_{Chem}$	ΔRE_{Chem}	$\Delta\epsilon_{Chem}$[a]
CuO/SiO_2	−1.9	2.8	−1.4	0.9	0.45	−1.45
Cu_2O/SiO_2	−0.4	2.2	−5.5	1.8	0.9	0.50

[a] $\Delta\epsilon_{Chem}$ accounts for the cfhanges in the initial state energy of the photoemitting atom. This considers both the density of charge at the copper site and the Madelung potential around it. Properly speaking the Madelung potential should be calculated by accounting for the effect of all the network atoms and not only the first neighbors. However, the effect of the second and further shells is comparatively small and is neglected here.

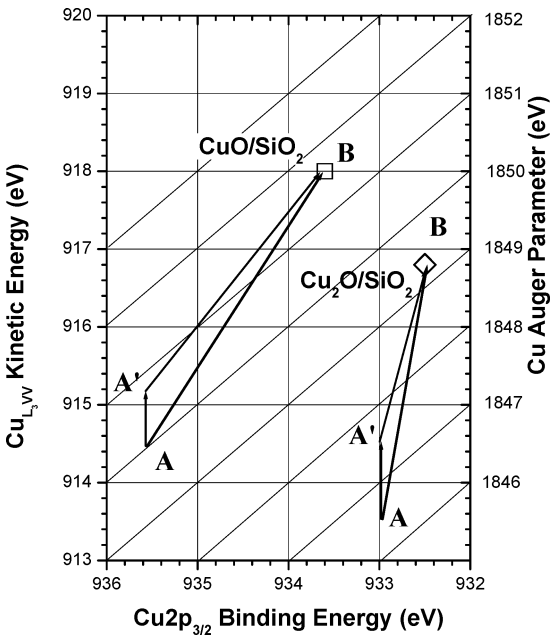

Figure 3. CSVs describing the polarization (vector **AA′**) and chemical (vector **A′B**) contributions to the experimental vector **AB** for the systems CuO/SiO_2 and Cu_2O/SiO_2.

the situation corresponding to Cu^+ and Cu^{2+} species tightly interacting with SiO_2 through the formation of Cu−O−Si cross-linking bonds at the interface, once discounting the difference in polarization. The change in coordinates of this new vector **A′B** reflects how the electronic parameters would vary in a Wagner plot because of the progressive change in the average chemical environment around the copper cations as a function of the size of the deposited moieties (i.e., from a Si−O−Cu to a Cu−O−Cu situation). Note that in an experiment of this kind this evolution is a result not only of the number of copper cations in each particular environment but also of the attenuation of the interface layers by those of the upmost zones of the deposited particles. The influence of the different chemical environments on the value of the electronic parameters will be modeled below by quantum mechanical calculations with clusters simulating the bonding of Cu^+ or Cu^{2+} at the interface or in the bulk.

Electronic Parameters and Coordination of Cations of Supported Metal Oxides. From studies with coordination compounds, it is known that XPS can be very sensitive to changes in the coordination state of the cations.[13,14] The problem that we want to address here is whether similar changes in coordination can also be monitored for metal cations present in very small oxide moieties deposited on the surface of another oxide substrate. In the context of the present investigation dealing with copper oxides, we have studied by XPS the adsorption of PA on the Cu_2O particles deposited on SiO_2. PA is well-known as a selective ligand of Cu^+ species.[30] The experiment carried out here consisted of the adsorption of that molecule on the Cu_2O/SiO_2 system when small amounts of the

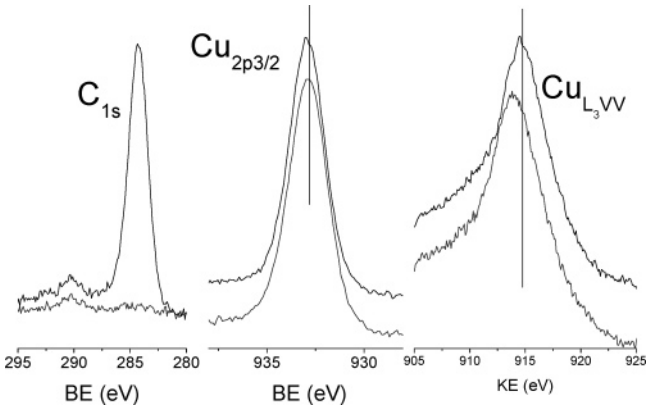

Figure 4. C 1s and Cu $2p_{3/2}$ photoelectron and Cu L_3VV Auger peaks before (bottom, line in gray) and after (top, line in black) adsorption of PA.

deposited phase (i.e., for a Cu/Si ratio of 0.054 as calculated from the areas of the Cu 2p and Si 2p peaks and their corresponding sensitivity factors). Figure 4 shows the C 1s, Cu 2p, and Cu L_3VV Auger peaks for the sample before and after the adsorption of the PA. It is apparent that, after adsorption, the intensity of the C 1s peak greatly increases and depicts a main peak characteristic of aliphatic and/or aromatic carbon. On the other hand, the Cu 2p photoelectron and Cu L_3VV Auger peaks change slightly in position and width (cf. Table 3), although keeping the shape and, for the Cu 2p photoelectron peak, the relative satellite/main peak intensity ratio. The state before adsorption corresponds to a point with the following coordinates in the Wagner plot (BE = 932.8, KE = 913.9), while the differences between values observed before adsorption minus those after adsorption amounted to $\Delta BE = -0.1$ eV and $\Delta KE = -0.8$ eV (i.e., $\Delta\alpha' = -0.9$ eV). The small difference between the BEs of the Cu 2p peaks was estimated after fitting two Gaussian curves to them. The difference found was of the order of 0.5−1.0 eV. For simplicity, we take this latter value for the discussion.

For higher Cu/Si ratios, the changes in the position of the photoemission and/or Auger peaks were smaller and, for the highest ratios, not detectable. This is attributed to the fact that the XPS signals of big Cu_2O particles are dominated by copper atoms that are not located at the Cu_2O/SiO_2 interface and, therefore, do not undergo any change due to the interaction with the PA.

The specificity of the PA interaction with Cu^+ containing surfaces is confirmed by the fact that the C 1s peak does not increase in intensity when a similar PA adsorption experiment was carried out on CuO/SiO_2 (i.e., a system where there are Cu^{2+} species in CuO particles dispersed on SiO_2). This result indicates that the PA ligand does not adsorb irreversibly on the free zones of the SiO_2 substrate or by direct interaction with Cu^{2+} species of bulk CuO. By contrast, similar variations in

TABLE 3: Change in Electronic Parameters of Copper by Adsorption of PA on Cu_2O/SiO_2 (All Values in eV)

state of the sample	Cu $2p_{3/2}$ BE	KE Auger peak	width at half-maximum Cu $2p_{3/2}$ (eV)	α'	$\Delta\alpha'_{ads}$[a]	$\Delta\epsilon_{ads}$[a]
before PA adsorption	932.8	913.9	2.5	1846.7		
after PA adsorption	932.9	914.7	2.1	1847.6	−0.9	−0.55

[a] Values calculated as differences between the situations before and after adsorption.

electronic parameters of copper were found when adsorbing PA on Cu_2O/ZrO_2 (i.e., Cu_2O deposited on a flat substrate of ZrO_2).[31]

Discussion

Initial and Final State Effects by the Photoemission of Cu^{n+} in Supported Cu_2O and CuO. A quantitative evaluation of the data in Tables 1 and 2 provides interesting hints to account for the local structure of the copper atoms at the interface and for the type of electronic interactions developing between copper oxide and SiO_2 support. The first obvious evidence is that the relaxation energy of the photoholes decreases for the atoms in close contact with the support (i.e., ΔRE 0.8 and 1.4_5 for CuO and Cu_2O, respectively). This behavior has been found for many other MO/M′O systems where M′O is a less polarizable material than MO. A detailed discussion of the reasons for such an effect can be found in refs 3 and 4 and will not be repeated in full here. The use of formula 3 permits one to calculate the difference in polarization energy of the media beyond the first coordination sphere around copper for small particles of the oxide dispersed on the support. This difference in polarization stems from the distinct intrinsic polarization of the media around the copper as depicted in Figure 2. Once this contribution has been calculated and subtracted from the experimental $\Delta\alpha'$ values tabulated in Table 1, the resulting parameters in Table 2 account for the effect of the oxygen ions at the first coordination sphere around the copper ions (i.e., bonding and chemical interactions). The positive values of ΔRE_{Chem} indicate that the relaxation energy of a photohole at the copper sites due to the first coordination sphere of atoms is always larger when the copper is in the bulk oxides than when it is directly interacting with the SiO_2 substrate. Another interesting feature is that the value of ΔRE_{Chem} is smaller for Cu^{2+} than for Cu^+.

On the other hand, the $\Delta\epsilon_{Chem}$ values in Table 2 have a positive (i.e., Cu_2O) and a negative (i.e., CuO) sign depending on the oxide. The change in ϵ_{Chem} indicates that there must be a change either in the local density of charge at the copper cations and/or in the MP around it when it is at the interface with the SiO_2. Referring to the Cu_2O/SiO_2 system, a positive value for $\Delta\epsilon_{Chem}$ would agree with a decrease in the positive charge at the copper sites and/or with an increase in the (negative) value of MP for the Si−O−Cu species with respect to the bulk Cu ions. It will be shown below by quantum mechanical calculations with several cluster models that in all cases the density of positive charge at the Cu^+ cations increases slightly when it bonds with oxygen ions at the interface. Therefore, we must attribute the positive sign of $\Delta\epsilon_{Chem}$ found for the Cu_2O/SiO_2 system to an increase in the negative value of MP, a feature that would be consistent with an increase in the coordination number of copper. For CuO we have found the opposite behavior (i.e., $\Delta\epsilon_{Chem} = -1.45$ eV). This indicates that either the density of positive charge at the Cu^{2+} ions is larger for the small particles of the oxide interacting with silica and/or that the (negative) value of MP around these ions is smaller than in bulk CuO. The quantum mechanical calculations reported below indicate that, for the different clusters considered for evaluation, there are not large changes in the density of charge at the copper sites. Therefore, we must admit that the (negative) value of MP around Cu^{2+} must be smaller for the supported oxide, a feature that would be consistent with a decrease in the coordination number of copper.

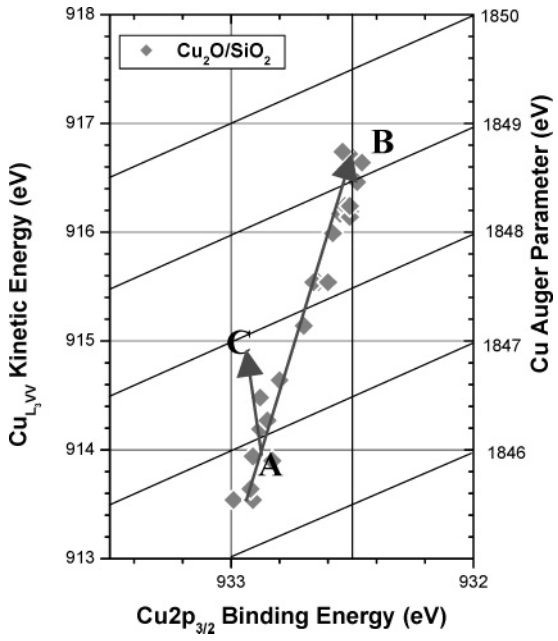

Figure 5. Wagner plot for the Cu_2O/SiO_2 system and CSV describing the effect of adsorbing PA (vector **AC**) on this system.

Ligand Effects for Coordinated Cu^+ Ions in Dispersed Cu_2O. The changes in the electronic parameters of copper upon bonding with the phenyl acetylene ligand can be schematically represented in a Wagner plot. Figure 5 shows, in the form of CSVs, the changes in electronic parameters between the points corresponding to bulk Cu_2O (B) and Cu_2O/SiO_2 before (A) and after (C) PA adsorption.

The changes in RE and ϵ between the points before and after adsorption (i.e., the difference between point A and point C) yields the values $\Delta RE_{ads} \sim -0.45$ and $\Delta\epsilon_{ads} \sim -0.55$ eV. The increase in RE after adsorption is attributed to an increase of the relaxation energy when Cu^+ is interacting with the PA ligand. Following the same arguments as before, the increase in ϵ must be attributed to either an increase in the density of positive charge and/or to a decrease in the negative value of the MP.

Quantum Mechanical Calculations with Cluster Models. For an experimental situation where small moieties of Cu_2O or CuO are deposited on SiO_2, it is reasonable to assume that most of the Cu^+ and Cu^{2+} species are bonded to oxide ions that act as a bridge between the copper oxide and the substrate. For systems such as Al_2O_3 deposited on SiO_2 we have previously found that the coordination state of the Al^{3+} cations at the interface can be different than in the bulk.[32] Here, as represented in Figure 6, we have considered a series of clusters to simulate the situation of copper in the bulk oxides (i.e., Cu_2O and CuO) or for the copper oxide interacting with the SiO_2 support. In the former case the bonding state of copper is simulated by assuming the formation of direct Cu−O−Cu bonds with a local

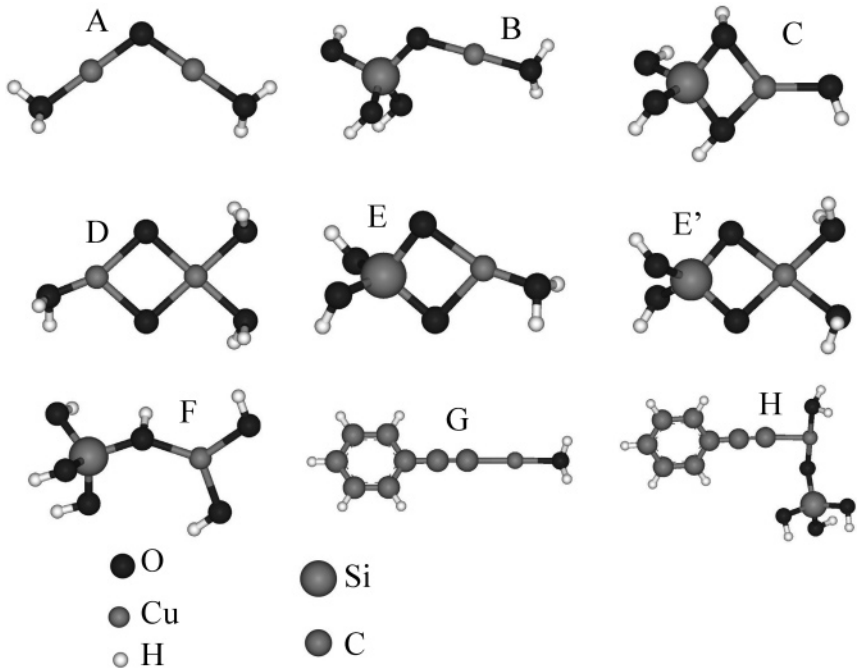

Figure 6. Structure of clusters proposed to describe the different states of copper at the interface with the silica and after adsorption of PA. A, B, and C correspond to Cu^+ species. D, E, and E′ correspond to Cu^{2+} species. G and H simulate the interaction of Cu^+ with PA. Atom symbols are indicated in the figure. Results from FD calculations for these atoms are reported in Table 4.

TABLE 4: Electron Densities, Relaxation Energies, and Charge Transfers Calculated for the Clusters Simulating the Photoemission from Copper Ions with Different Local Coordinations

cluster	structure (initial state)	ρ^a	$\Delta\rho^b$	structure (final state)	r	$\Delta\rho^c$	RE_{Chem} (eV)	$\Delta RE_{Chem}{}^c$ (eV)	$\Delta q^{M\,d}$
Cu(I) A	(O)CuOCu	10.45		(O)ZnOCu	10.69		804.15		0.24
Cu(I) B	(O)CuOSi	10.31	0.14	(O)ZnOSi	10.49	0.20	802.66	1.49	0.18
Cu(I) C	OCu(2O)Si	10.07	0.38	OZn(2O)Si	10.33	0.36	803.26	0.89	0.24
Cu(I) G	(O)Cu-AP	10.43	0.02 (−0.36)	(O)Zn-AP	10.61	0.08	803.11	1.04	0.18
Cu(I) H	(O,AP)Cu(O)Si	10.41	0.04 (−0.34)	(O,AP)Zn(O)Si	10.63	0.06	808.77	4.62	0.22
Cu(II) D[e]	(2O)Cu(2O)Cu	10.02		(O)Zn(2O)Cu	10.45		804.41		0.43
Cu(II) D′[e]	(O)Cu(2O)Cu	9.88		(2O)Zn(2O)Cu	10.49		804.47		0.57
Cu(II) E	(O)Cu(2O)Si	9.91	0.11	(2O)Zn(2O)Si	10.38	0.07	802.03	2.38	0.47
Cu(II) E′	(2O)Cu(2O)Si	9.74	0.28	(2O)Zn(2O)Si	10.15	0.30	802.50	1.91	0.41
Cu(II) F	(2O)Cu(O)Si	9.68	0.34	(O)Zn(2O)Si	10.33	0.12	803.03	1.38	0.65

[a] Electronic density calculated by the sum of the 3d + 4s + 4p electron populations. [b] $\Delta\rho$ is calculated by subtraction of ρ(A) − ρ(B, C, G, or H) and ρ(D) − ρ(E, E′, or F). For clusters G and H, the values in parentheses have been calculated by subtraction: ρ(C) − ρ(G or H). [c] ΔRE is calculated by subtraction of RE(A) − RE(B, C, or H) and RE(D) − RE(E or F). [d] Δq^M for each row is calculated by subtracting the value of ρ for clusters XCuX minus that of XZnX. [e] Calculations are done for three (D′) and four (D) coordinated Cu^{2+} species in CuO.

structure (bond angles and distances) similar to that existing in the lattice of the bulk compounds. For the copper oxides interacting with the SiO_2 surface, the clusters consist of a SiO_2 tetrahedron bonded to Cu^+ or Cu^{2+} ions which are coordinated to other oxide ions as in the bulk oxides. We have assumed that the copper species might be bonded to the SiO_2 surface through either one or two oxide ions (in general we will refer in the following to these two situations as Si−O−Cu). This accounts for the possibility that the local arrangement (and therefore the MP) around copper changes upon interaction with the substrate material. For all the clusters we have calculated the energy in their initial state and in their final state, before and after photoemission. In this latter case we have used the $Z + 1$ approximation (i.e., the Cu^{n+} ion has been substituted by a $Zn^{(n+1)}$ ion while leaving frozen the geometry of the clusters). The relaxation energy in the final state (intra- and extra-atomic) can be estimated to be equivalent to the energy of these Zn^{n+1} clusters, while the difference in extra-atomic energy between the bulk and the highly dispersed copper oxides interacting with the silica (i.e., ΔRE_{Chem}) can be estimated as the difference between the energies of the Cu−O−Cu and Si−O−Cu clusters in their final states. Table 4 reports all these energetic terms, together with other interesting parameters like the electron occupancy of the shallow valence levels of copper (i.e., sum of the 3d+4p+4s electron populations, referred in Table 4 as ρ) and the differences in electron density at the copper sites between the Cu−O−Cu and Si−O−Cu situations (i.e., $\Delta\rho$). The density of charge transferred from the oxygen ions to the copper upon creation of a hole by photoemission (i.e., in the $Z + 1$ state) is also included in the table (i.e., Δq^M). In all cases, a migration of charge from the oxygen ligands to the copper occurs upon photoemission. The magnitude of this migration depends on the type of cluster and ranges between 0.24 and 0.48 electrons. A net transfer of charge from the oxide ligands to the metal centers after the ejection of a photoelectron is commonly accepted as the main relaxation mechanism in oxides.[33]

Table 4 shows that ρ (Cu^+) is always smaller for the Si−O−Cu clusters. This must be due to the fact that the Cu−O−Si bridging bond is more covalent and detracts electron density from the copper sites (the density of positive charge would therefore increase at the copper). This would contribute to make

$\Delta\epsilon_{Chem}$ negative, the opposite to what is determined experimentally (i.e., $\Delta\epsilon_{Chem} = 0.5$ eV, Table 2). Therefore, the positive value of $\Delta\epsilon_{Chem}$ supports that upon interaction with the silica surface, the (negative) MP around copper increases with respect to the bulk oxide. Such a change is congruent with an increase in the coordination number around copper in the Si−O−Cu state. Table 4 reports calculated data for two clusters simulating the Cu_2O/SiO_2 interface, where Cu^+ is bonded to two (cluster B) or three (cluster C) oxide ions. In this latter case two oxide ions act as bridges with the SiO_2 substrate. For the two clusters the calculated $\Delta\rho$ values are positive. Since for cluster C the (negative) value of the MP must be larger, we assume that this is the cluster that best describes the coordination state of Cu^+ at the interface with the SiO_2. A further point in favor of that structure is the fact that the calculated and experimental ΔRE_{Chem} values are very similar (cf. Tables 2 and 4).

The situation for CuO is the opposite. The sign of the experimentally determined $\Delta\epsilon_{Chem}$ (cf. Table 2) is negative and its magnitude rather high. The calculated $\Delta\rho$ for the CuO/SiO_2 clusters are positive a feature that agrees with the negative sign of $\Delta\epsilon_{Chem}$. However, the large (negative) value of this parameter ($\Delta\epsilon_{Chem} = -1.45$ eV) would be hardly justified by the calculated $\Delta\rho$ values. Therefore, we tentatively assume that copper atoms at the interface must have a smaller (negative) MP and that their bonding structure must be similar to that of clusters E or F with a coordination number of three and either one or two oxygen ions bridging to the silicon. Calculated ΔRE values in Table 4 for Cu(II) clusters are all positive, a fact that agrees with the experimentally determined values. The obtained values are 1.91 for cluster E′, with a coordination number of 4, and 2.38 and 1.38 eV for clusters E and F, with a coordination number of 3. The calculated values for cluster F is closer to that determined experimentally (cf. Table 2), a fact that supports that the coordination state of copper in this cluster must be closer to the actual state of copper at the interface.

Adsorption of PA on the Cu_2O/SiO_2 system leads to the following changes in electronic parameters with respect to the bulk oxide: $\Delta\epsilon = 0.45$ and $\Delta RE = 0.85$ eV. This means that the extra-atomic relaxation energy varies according to $Cu_2O > Cu_2O/SiO_2-PA > Cu_2O/SiO_2$. From the two cluster models of PA interacting with Cu^+ species whose calculated parameters are summarized in Table 4, only the calculated ΔRE value for cluster G (for simplicity, in this structure the effect of SiO_2 has not been considered in the calculations) is similar to the experimental value. Thus, a likely picture would be that upon adsorption of PA, this molecule interacts directly with Cu^+ ions bonded to one oxide ion (total coordination number two). This cluster structure yields a value of $\Delta\rho < 0$ when compared to the state before adsorption (i.e., cluster C, values in parentheses in Table 4) and has a smaller MP than this latter (in cluster G copper is only bonded to one oxygen and one carbon atoms). The differences in these two magnitudes are in agreement with the experimentally determined ΔRE_{ads} ($\Delta RE_{ads} = \Delta\alpha'/2$) and $\Delta\epsilon_{ads}$ (cf. Table 3).

Conclusions

The present work is the continuation of a series of investigations by means of XPS of different MO/M′O systems.[3] Here, we have intended a deeper understanding of the changes of electronic parameters when copper oxides in the form of nanometric clusters are strongly interacting with the support. The results obtained with copper oxide moieties highly dispersed on the surface of silica and its interpretation with quantum mechanical calculations with cluster models have provided some clues to correlate the photoemission events with the local structure of copper ions.

XPS has been traditionally used for the characterization of the oxidation state of cations and, less commonly, the coordination structures of elements in solids. In general, the most common practice is to associate a given oxidation state/type of compound with a certain binding energy and Auger parameter values. Our results here and in previous publications[3,4,7,11,32] show that very large difference in these parameters can be found when the dispersion degree is high. In the present work, we have gone a step forward for the understanding of the factors that control these changes. The quantum mechanical calculations with cluster models have provided a reasonable description of the different energetic terms involved in the photoemission process. From this description, we have been able to propose some possible coordination states for Cu^+ and Cu^{2+} species in their respective copper oxides when they are interacting with SiO_2. Moreover, we have shown that Cu^+ species at the surface of SiO_2 may interact with an organic ligand as PA and that, as a result of this interaction, there are changes in the electronic parameters of copper and in its coordination state

Acknowledgment. We thank the Mto. de Ciencia y Tecnología of Spain (Projects PPQ 2001-3108 and CTQ 2004-00582/BQU) for financial support and Drs P. Palma and J. Campora from the Instituto de Investigaciones Quimicas (CSIC-University Sevilla) for a supply of the phenyl acetylene compound.

References and Notes

(1) Wagner, C. D. *Faraday Discuss. Chem. Soc.* **1975**, *60*, 291.
(2) Moretti, G. *J. Electron Spectroscopy Relat. Phenom.* **1998**, *95*, 95.
(3) Gonzalez-Elipe, A. R.; Yubero, F. Spectroscopic Characterization of oide−oxide Interfaces. In *Handbook of Surfaces and Interfaces of Materials*; Nalwa, H. S., Ed.; Academic Press: London 2001; Vol, 2, Surface and Interface Analysis and Properties; p 147.
(4) Mejias J. A.; Jimenez, V. M.; Lassaletta, G.; Fernandez, A.; Espinos, J. P.; Gonzalez-Elipe, A. R. *J. Phys. Chem.* **1995**, *100*, 1484.
(5) Bertoti, I.; Mink, G.; Szekely, T.; Varsanyi, G.; Reti, F. *Surf. Interface Anal.* **1986**, *9*, 237.
(6) Yubero, F.; Stabel, A.; Gonzalez-Elipe, A. R.; *J. Vac. Sci. Technol. A* **1998**, *16*, 3477.
(7) ,. Morales, J.; Caballero, A.; Holgado, J. P.; Espinos, J. P.; Gonzalez-Elipe, A. R.; *J. Phys. Chem.* **2002**, *106*, 10185.
(8) Stott, F. H. *Rep. Prog. Phys.* **1987**, *50*, 861.
(9) Berdnorz, J. G.; Muller, K. A. Z. *Physica B* **1986**, *64*, 189.
(10) Fleisch, T. H.; Mains, G. J. *Appl. Surf. Sci.* **1982**, *10*, 51.
(11) Espinos, J. P.; Morales, J.; Barranco, A.; Caballero, A.; Holgado, J. P.; Gonzalez-Elipe, A. R. *J. Phys. Chem. B* **2002**, *106*, 6921.
(12) Moretti, G.; Filippone, F.; Satta, M. *Surf. Interface Anal.* **2001**, *31*, 249.
(13) Sharma, C. V. K.; Chusuei, C. C.; Clerac, R.; Moller, T.; Dunbar, K. R.; Clearfield, A. *Inorg. Chem.* **2003**, *42*, 8300.
(14) Horton, J. H.; Rasmusson, J.; Shapter, J. G.; Norton, P. R. *Can. J. Chem.* **1998**, *76*, 1559.
(15) Barranco, A.; Yubero, F.; Espinós, J. P.; A. R. González-Elipe, A. R.; *Surf. Interface Anal.* **2001**, *31*, 761.
(16) Parr, R. G. Wang, W. *Density-functional theory of atoms and molecules*; Oxford University Press: Oxford, U.K., 1989.
(17) Becke, A. D. *J. Chem. Phys.* **1993**, *98*, 5648.
(18) Dunning, T. H., Jr.; Hay, P. J. In *Modern Theoretical Chemistry*; Schaefer, H. F., III.; Plenum: New York, 1976; Vol. 3, pp 1−28.
(19) Wedig, U.; Dolg, M.; Stoll, H.; Preuss, H. In *Quantum Chemistry: The Challenge of Transition Metals and Coordination Chemistry*; Veillard, A., Ed.; Reidel: Dordrecht, The Netherlands, 1986; p 79.
(20) Reed, A. E.; Curtiss, L. A.; Weinhold, F. *Chem. Rev.* **1988**, *88*, 899.
(21) Krishnan, R.; Binkley, J. S.; Seeger, R.; Pople, J. A. *J. Chem. Phys.* **1980**, *72*, 650.
(22) Wachters, J. H. *J. Chem. Phys.* **1970**, *52*, 1033.
(23) Hay, P. J. *J. Chem. Phys.* **1977**, *66*, 4377.
(24) Raghavachari, K.; Trucks, G. W. *J. Chem. Phys.* **1989**, *91*, 1062.
(25) Clark, T.; Chandrasekhar, J.; Spitznagel, G. W.; Schleyer, P.v. R. *J. Comput. Chem.* **1983**, *4*, 294.

(26) Frisch, M. J.; Pople, J. A.; Binkley, J. S. *J. Chem. Phys.* **1984**, *80*, 3265.

(27) Frisch, M. J.; Trucks, G. W.; Schlegel, H. B.; Scuseria, G. E.; Robb, M. A.; Cheeseman, J. R.; Montgomery, J. A., Jr.; Vreven, T.; Kudin, K. N.; Burant, J. C.; Millam, J. M.; Iyengar, S. S.; Tomasi, J.; Barone, V.; Mennucci, B.; Cossi, M.; Scalmani, G.; Rega, N.; Petersson, G. A.; Nakatsuji, H.; Hada, M.; Ehara, M.; Toyota, K.; Fukuda, R.; Hasegawa, J.; Ishida, M.; Nakajima, T.; Honda, Y.; Kitao, O.; Nakai, H.; Klene, M.; Li, X.; Knox, J. E.; Hratchian, H. P.; Cross, J. B.; Adamo, C.; Jaramillo, J.; Gomperts, R.; Stratmann, R. E.; Yazyev, O.; Austin, A. J.; Cammi, R.; Pomelli, C.; Ochterski, J. W.; Ayala, P. Y.; Morokuma, K.; Voth, G. A.; Salvador, P.; Dannenberg, J. J.; Zakrzewski, V. G.; Dapprich, S.; Daniels, A. D.; Strain, M. C.; Farkas, O.; Malick, D. K.; Rabuck, A. D.; Raghavachari, K.; Foresman, J. B.; Ortiz, J. V.; Cui, Q.; Baboul, A. G.; Clifford, S.; Cioslowski, J.; Stefanov, B. B.; Liu, G.; Liashenko, A.; Piskorz, P.; Komaromi, I.; Martin, R. L.; Fox, D. J.; Keith, T.; Al-Laham, M. A.; Peng, C. Y.; Nanayakkara, A.; Challacombe, M.; Gill, P. M. W.; Johnson, B.; Chen, W.; Wong, M. W.; Gonzalez, C.; Pople, J. A. *Gaussian 03*, revision B.04; Gaussian, Inc.: Pittsburgh, PA, 2003.

(28) Carniato, S.; Dufour, G.; Luo, Y.; Ågren, H. *Phys. Rev. B* **2002**, *66*, 045105.

(29) Thomas, T. D. *J. Electrón Spectrosc. Relat. Phenom.* **1980**, *20*, 117.

(30) Abel, E. W., Gordon, F., Stone, A., Willkinson, G., Eds. *Comprehensive Organometallic Chemistry II. A review of the literature 1982−1994*; Pergamon Press: Oxford, U.K., 1995; Wardell, J. L., Ed., Vol. 3, Copper and Zinc Groups; p 67.

(31) Morales, J.; Espinos, J. P.; Caballero, A.; Gonzalez-Elipe, A. R.; Unpublished results.

(32) Reiche, R.; Yubero, F.; Espinos, J. P.; Gonzalez-Elipe, A. R. *Surf. Sci.* **2000**, *457*, 199.

(33) Veal, B. W.; Paulikas, A. P. *Phys. Rev. B* **1985**, *31*, 5399.